JOURNAL OF MATERIALS SCIENCE 20 (1985) 3150 – 3156

Microindentation analysis of di-ammonium hydrogen citrate single crystals

JOY GEORGE, GEORGE PETER
Solid State Physics Laboratory, Department of Physics, University of Cochin, Cochin 682 022, India

Microindentation analysis of di-ammonium hydrogen citrate single crystals is reported here for the first time. The single crystals grown by a slow evaporation method are indented on the as-grown (0 0 1) and cleavage (1 1 0) faces using a diamond pyramid indenter, and the hardness variation with load is studied. The toughness is determined by measuring the crack length. The values of hardness and toughness are used to evaluate the brittleness of these crystal faces. The crack system formed around the indentations is analysed by etching and surface removal techniques, and it is shown that the threshold crack is radial. As the indentation load is increased, lateral cracks initiate and take the shape of median cracks with further increase in load.

1. Introduction

Many organic crystals belonging to the orthorhombic class exhibit ferroelectric [1], electro-optic [2] and triboluminescent [3] properties. Although triboluminescence is an old phenomenon, relatively little progress has been made in the study of it because of the complexity of crystal fracture. Di-ammonium hydrogen citrate, $C_6H_{14}N_2O_7$, (hereafter termed DAHC) single crystals, which belong to the orthorhombic system with space group *Pn2b* with lattice parameters $a = 1.0767\,\text{nm}$, $b = 1.4736\,\text{nm}$, $c = 0.6165\,\text{nm}$ and four molecules per unit cell [4] are reported to be piezoelectric and triboluminescent [5]. No data are available on the deformation and fracture characteristics of the DAHC crystal, and so it was thought useful to make a microindentation analysis to study the hardness and toughness, and to evaluate the brittleness factor of this crystal.

Hardness, though a poorly defined term, usually implies resistance to deformation which in turn denotes the ability of one body to resist penetration by another. It depends on the elastic and plastic properties of both the indenter and the indented material. Among the various methods for hardness measurement, the most common method is the microindentation method and pyramid indenters are said to be best suited for hardness tests due to two reasons [6], namely (a) the contact pressure for a pyramid indenter is independent of indent size, and (b) pyramid indenters are less affected by elastic release than other indenters. The Vickers pyramid indenter, whose opposite faces contain an angle of 136°, is the most widely accepted pyramid indenter. Using a Vickers indenter, the hardness of any material is determined employing the equation $P/a^2 = \alpha H$, where P is the load, a is half the diagonal of the impression, α is an indenter constant whose value best fitted to available experimental data is 2 [7], and H is the hardness value.

Toughness of a material denotes its resistance to fracture. As the indentation load is increased, cracks are initiated in the indented material around the indenter and these cracks propagate on subsequent loading. Of the two processes of initiation and propagation, the latter has received considerable attention. However,

0022–2461/85 $03.00 + .12

models have been proposed [8, 9] to predict the critical load and flow size conditions which should prevail at the threshold of crack initiation. With the development of Griffith–Irwin fracture mechanics, several parameters have become available for specifying resistance to crack growth. Of these, the fracture toughness, K_c has gained the widest acceptance as a material quantity in design. In terms of fracture mechanics, the toughness parameter is interpreted physically at two levels [10]. Macroscopically, it emerges as a composite of elastic and surface formation properties, and microscopically it relates to the basic nonlinear separation process responsible for crack tip extension. For a solid containing a well developed crack of specified dimension, K_c determines the fracture stress in uniform tensile loading and is accordingly a key material quantity in strength analysis. The usefulness of toughness as a fracture parameter is explicit in some of the applications in ceramic engineering [11].

Among a large variety of experimental methods available for measurement of toughness [11–15], the indentation method is the best suited for brittle materials with low toughness value. This is due to the simplicity and rapidity with which toughness can be evaluated using small samples. Analysis of the deformation/fracture mechanics of the indentation process has provided an equilibrium relation for the characteristic dimension c (half the crack length) for the propagation stage, assuming that a well-developed median crack extends under centre-loading conditions as $P/c^{3/2} = \beta_0 K_c$ $(c \geqslant a)$, where β_0 is an indenter constant. The value of this constant best fitted to the data is 7 [7] for a Vickers indenter. (Fig. 1).

Though the process of crack initiation is highly complex, the key feature of the $c(P)$ function appropriate to the initiation stage of a crack is a minimum in the load at $P^* = \lambda_0 K_c (K_c/H)^3$, with a characteristic $c^* = \mu_0 (K_c/H)^2$, where λ_0 and μ_0 are constants whose value best fitted to experimental data are 1.6×10^4 and 120 respectively, as given by Lawn and Marshall [7].

Direct observation of the indentation process has shown that the radial cracks attached to the corners of the indentation mark start from favourable surface flaws [16] in the near-surface plastic zone. The lateral cracks are understood to start from favourable sub-surface flaws at the elastic–plastic boundary, and are propagated by the rather high tensile unloading stress [17–20]. The median cracks initiate from sub-surface nucleation centres in the vicinity of the elastic–plastic boundary under the tensile stress of indentation stress fields [21]. The subsequent propagation is believed to be due to the wedging action of the indenter.

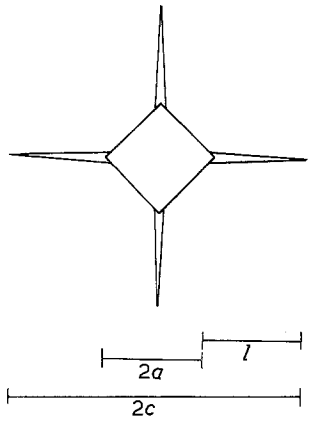

Figure 1 Schematic diagram showing a cracked microindentation impression.

Brittleness, which in a general sense implies the relative susceptibility of a material to two competing mechanical responses, deformation and fracture, is an important property as far as the mechanical behaviour of a material is concerned. It depends on various factors like temperature, rate of loading and atmosphere. Lawn and Marshall [7] have suggested the indentation technique to evaluate the largely empirical brittleness factor of a material, taking the ratio H/K_c as a simple index to brittleness with a view to providing a basis for material classification.

The indentation analysis presented in this paper consists in (a) the study of the variation of hardness with load on (0 0 1) and (1 1 0) planes using a Vickers pyramidal indenter; (b) analysing the validity of the equilibrium relation at the propagation stage of the crack and showing that the radial crack is the threshold event in crack formation; and (c) determining the value of H/K_c as a simple index of brittleness for classifying DAHC crystals.

2. Experimental details

DAHC single crystals were grown from aqueous solution at constant temperature by slow evaporation. The crystals were then taken out,

washed and dried. Indentations were made on the as-grown (0 0 1) face with the indenter diagonal along [0 1 0] and [1 0 0] directions, and on the cleavage (1 1 0) face with the indenter diagonal along [$\bar{1}$ 1 0] and [0 0 1] directions. These indentations were made on dislocation-free regions using a Hanemann microhardness tester Model D32. In this model a Vickers pyramid diamond indenter is fixed to the front lens of the reproducing objective, whose optical data are those of standard $32\times/0.65$ apochromats. The hardness tester, which is provided with an optical device to indicate the testing load, was attached to an incident-light microscope (Epityp 2, Carl Zeiss, Jena), with the vertical illuminator replacing a standard objective. An indentation load as low as 0.2 g can be used for this model, which makes the study of the deformation and fracture of materials possible at low loads. The indentation impression was measured using a micrometer eyepiece which resembled the standard micrometer eyepiece in design, with a least count of 10 μm. For the measurement of the diagonal of the impression and the length of the crack a high-power objective was used in the place of a reproducing objective of the indenter. A number of samples (approximately 10 mm × 3 mm × 2 mm) were indented and corresponding to different loads in the range of interest, at least ten indentations were made and the average diagonal length of the indentation obtained for each load. At first the load was applied for a time $T = (t_s + t)$, where $t_s = 5$ sec is the sinking time of the diamond pyramid, varying the actual load resting time t from 5 to 300 sec at constant load. The permanent impressions for these and subsequent trials were measured after a time lapse of 30 min to allow for any elastic recovery. Since the area of the impression did not bear any observable dependence on loading time for the constant load used, t was taken as 15 sec for all subsequent trials.

To study the nature of the threshold crack on (0 0 1) and (1 1 0) faces, the indented specimens were viewed under an optical microscope for different loads from 0.5 g to the point when well-developed cracks formed. The indented surface was also observed after etching with a suitable etchant to detect the initiation of cracks. To confirm the above observations, another set of indentations in the same load range was made and the surface studied under a microscope after gradual surface removal.

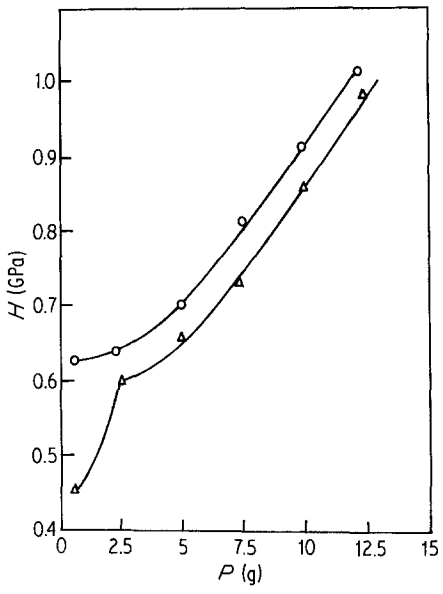

Figure 2 Variation of hardness with load in the load region 0.5 to 12.5 g: △, (0 0 1) face; ○, (0 1 0) face.

3. Results and discussion

The variation of hardness with load is given in Fig. 2. Values of load up to 12.5 g are used for hardness measurements, since the incidence of cracking does not seem to influence the deformation mechanics as long as the impression remains reasonably well defined and the crack does not extend considerably compared to the impression diagonal [22]. The special feature of the variation is the sharp increase in hardness with increase in load. The major contribution to the increase in hardness with load in DAHC is attributed to the high stress required for homogeneous nucleation of dislocations in the small dislocation-free regions indented [23]. Also in the case of DAHC, microcracks ($c < a$) appear below 12.5 g. Thus a part of the applied stress is utilized for nucleation and propagation of these cracks and does not contribute to any increase in deformed area beneath the indenter, resulting in an increase in hardness value.

For loads greater than about 12.5 g the cracks are large compared with the impression diagonal, and hence the toughness parameter comes into play. The plot of P against $c^{3/2}$ for loads up to 25 g, where the slope suddenly changes, is shown in Fig. 3. Loads beyond 25 g were not used for the evaluation of toughness as

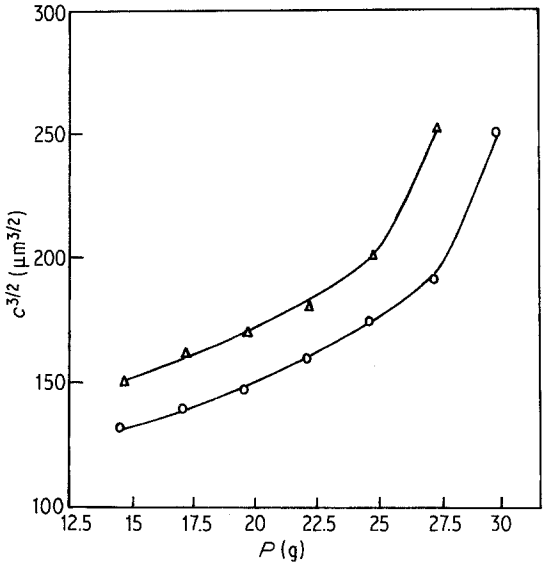

Figure 3 Variation of 2/3 power of semicrack length with load: △, (0 0 1) face; ○, (1 1 0) face.

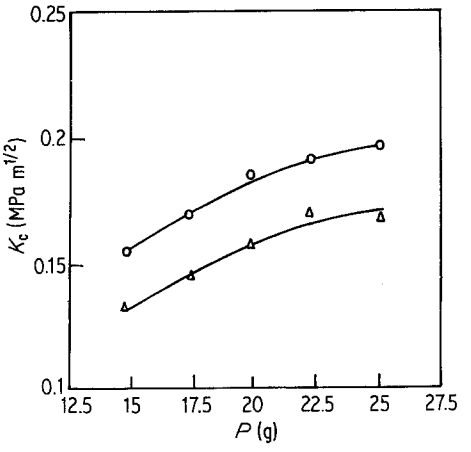

Figure 5 Variation of toughness with load: △, (0 0 1) face; ○, (1 1 0) face.

chipping of material occurs sometimes above this load. Niihara [24] has suggested the Palmqvist crack length l (Fig. 1) instead of the median crack length c in the low-load region for the evaluation of fracture toughness, and recommends $1/a$ as a more appropriate normalization parameter than c/a for toughness evaluation. But in the case of DAHC single crystal for loads above 12.5 g well-developed median cracks are formed (Fig. 4) although $c/a \sim 2$ to 5. The preference of c over l in the present case is further supported by Lankford [25] who has shown that the c/a normalization parameter "most nearly approaches universality".

The toughness value calculated is found to increase with increase in load in a regular manner as seen from Fig. 5. The hardness, toughness and brittleness values for (0 0 1) and (1 1 0) faces are given in Table I. For the purpose of classification and comparison with the corresponding values of well-known materials, the average values of hardness, toughness and brittleness for the two planes is calculated and presented in Table II. This procedure is justified since there is no remarkable variation in these values for the two planes investigated, and the directional dependence of hardness and toughness is negligibly small.

Chemical etching is a useful technique by which slip traces and crack system around a microindentation can be easily observed. In order to show that cracks, if they are formed due to indentation, should be visible under the microscope, two indentation marks, one with visible cracks (Fig. 6a) and the other without visible cracks (Fig. 7a) on the (0 0 1) face were etched with a suitable etchant. The position of the

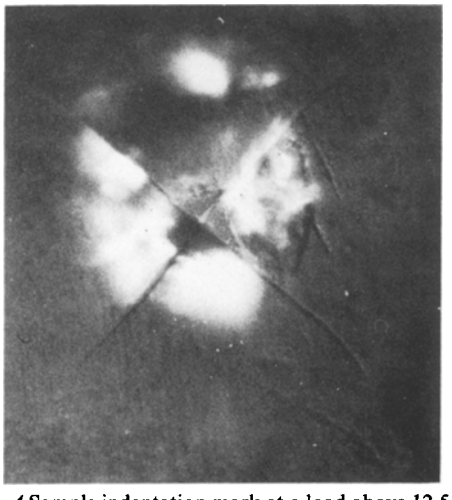

Figure 4 Sample indentation mark at a load above 12.5 g on (0 0 1) face, showing halfpenny configuration around the indentation mark.

TABLE I Hardness, toughness and brittleness of DAHC

Faces	Load range (g)	Hardness (GPa)	Toughness (MPa m$^{1/2}$)	Brittleness (μm$^{-1/2}$)
(0 0 1)	0.5 to 12.5	0.628	–	–
	12.5 to 25.0	–	0.154	4.08
(1 1 0)	0.5 to 12.5	0.738	–	–
	12.5 to 25.0	–	0.185	3.99

TABLE II Hardness, toughness, brittleness and threshold load and crack length values of DAHC presented with the corresponding values of some well-known materials

Material	Deformation/fracture parameters			Threshold parameters			
	Hardness (GPa)	Toughness ($MPa\,m^{1/2}$)	Brittleness ($\mu m^{-1/2}$)	Load (theory) (N)	Load (experiment) (N)	Crack length (theory) (μm)	Crack length (experiment) (μm)
NaCl*	0.24	0.5	0.48	7.11	14.7	120.0	100.0
$C_6H_{14}N_2O_7$	0.68	0.17	4.04	0.04	0.04	7.43	6.1
ZnSe†	1.1	0.9	1.2	8.0	–	80.0	–
ZnS†	1.9	1.0	2.0	2.0	–	30.0	–
Fe†	5.0	50.0	0.1	800 000	–	12 000	–
MgF_2†	5.8	0.9	6.0	0.05	–	3.0	–
SiO_2†	6.2	0.7	9.0	0.02	–	1.5	–
Ge*	9.0	0.46	19.56	0.01	0.02	0.14	0.25
Si*	10.0	0.6	16.66	0.02	0.04	0.2	0.65
Al_2O_3*	12.0	4.0	3.0	0.25	0.24	5.0	3.0
Si_3N_4†	16.0	5.0	3.0	2.0	–	12.0	–
SiC*	19.0	4.0	4.7	0.07	0.09	2.0	1.0
WC†	19.0	13.0	1.4	70.0	–	60.0	–

*Data from Lankford [25].
†Data from Lawn and Marshall [7].

cracks visible earlier in the indentation marks are now shown by the four arms at the corners (Fig. 6b) whereas the indentation without visible cracks shows no trace of cracks (Fig. 7b). Fig. 8a shows two indentation marks with cracks at different loads. After removal the crack lines have disappeared (Fig. 8b), which clearly indicates that the cracks are radial and originate from the surface. For the smaller load, only radial cracks are formed indicating that a radial crack is the threshold event in crack formation in DAHC. As the load is increased lateral cracks are observed around the impression (Fig. 9a). The lateral crack system is clearly seen in the etched pattern (Fig. 9b). The lateral cracks seem to extend well below the plane of indentation pyramidal apex, as can be seen from Fig. 9c, where the indentation impression is completely removed; the cracked area is still visible. At higher loads lateral cracks take the shape of

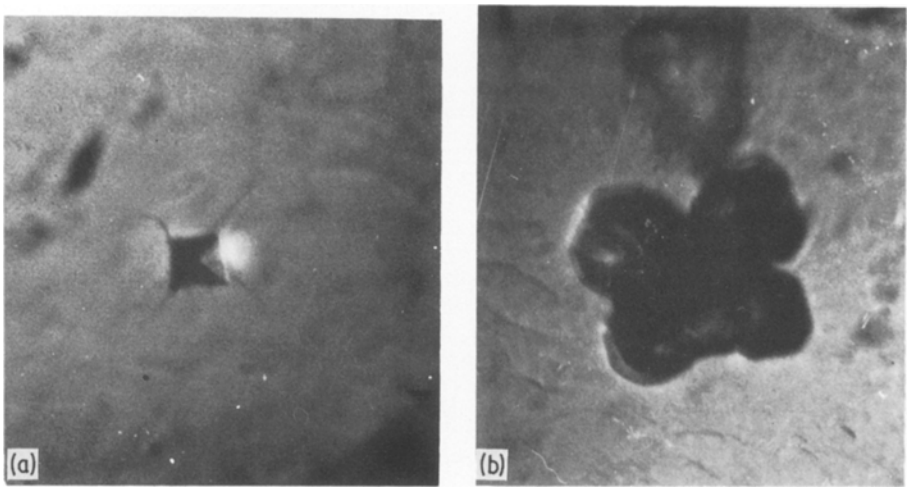

Figure 6 (a) Indentation micrographs showing threshold cracks on (0 0 1) face; (b) etch figure of the indentation mark in (a), showing four arms in the directions of the cracks.

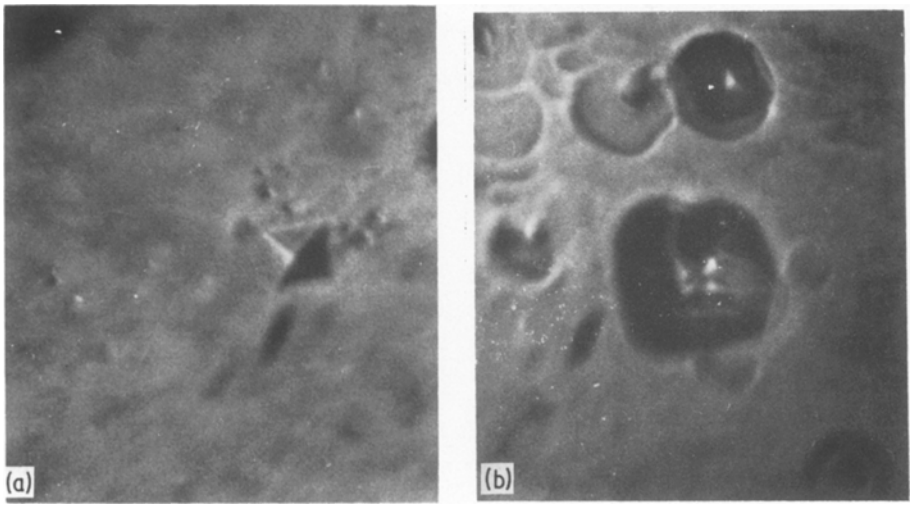

Figure 7 (a) An indentation mark at the threshold load without any visible crack; (b) etch figure of the indentation mark in (a) which verifies the absence of a crack.

median cracks, forming a well-developed half-penny configuration around the indentation mark (Fig. 4).

4. Conclusions

1. Hardness, toughness and brittleness values of DAHC are found to be 0.68 GPa, 0.17 MPa $m^{1/2}$ and 4.04 $m^{-1/2}$ respectively.

2. The hardness and toughness of DAHC are found to vary with load.

3. The threshold crack in the case of DAHC is radial, growing into lateral and median cracks as the load is increased step by step.

Acknowledgements

One of the authors (G.P.) is grateful to the University Grants Commission, India, for awarding a Teacher Fellowship and to the management of Sacred Heart College, Thevara, for sanctioning leave.

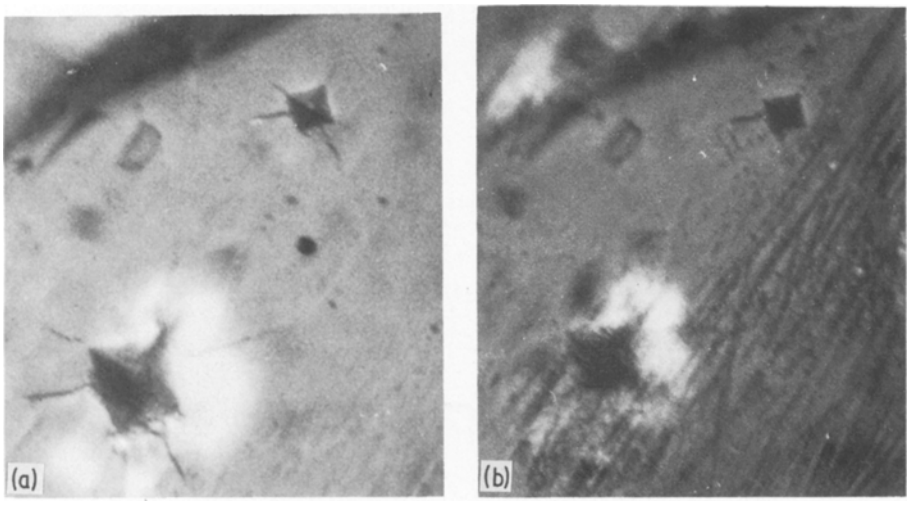

Figure 8 (a) Indentation marks at two different loads showing the crack system on the (0 0 1) face; (b) the area in (a) after surface removal.

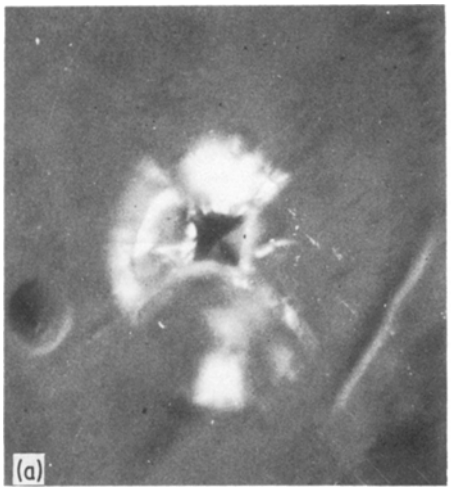

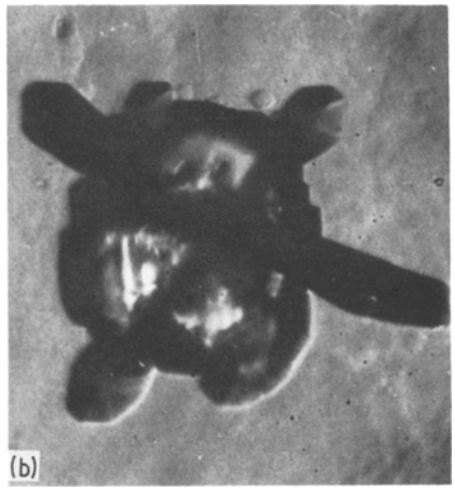

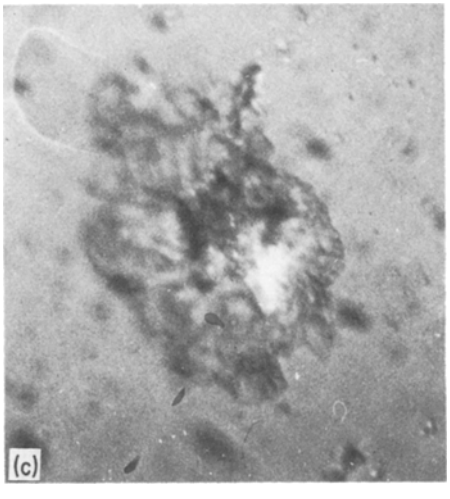

Figure 9 (a) An indentation mark showing lateral cracks on the (0 0 1) surface; (b) etch figure of lateral cracks on the (0 0 1) face showing the crack system clearly; (c) the area seen in (a) after surface removal, indicating that the cracks have extended well below the pyramidal apex of the indentation impression.

References

1. C. J. GOLDSMITH and J. G. WHITE, *J. Chem. Phys.* **31** (1959) 1175.
2. J. L. STEVENSON, *J. Phys. D, Appl. Phys.* **6** (1973) L13.
3. J. I. ZINK and W. KLIMT, *J. Amer. Chem. Soc.* **96** (1974) 4690.
4. W. E. LOVE and A. L. PATTERSON, *Acta Crystallogr.* **13** (1960) 426.
5. B. P. CHANDRA and M. ELYAS, *J. Phys. C.* **12** (1979) L695.
6. F. J. BALTA-CALLEJA, D. R. RUEDA, R. S. PORTER and W. T. MEAD, *J. Mater. Sci.* **15** (1980) 765.
7. B. R. LAWN and D. B. MARSHALL, *J. Amer. Ceram. Soc.* **62** (1979) 347.
8. B. R. LAWN and A. G. EVANS, *J. Mater. Sci.* **12** (1977) 2195.
9. J. T. HAGAN, *ibid.* **14** (1979) 2975.
10. B. R. LAWN and T. R. WILSHAW, "Fracture of Brittle Solids" (Cambridge University Press, London, 1975) Chs. 3 and 4.
11. A. G. EVANS, "Fracture Mechanics of Ceramics", Vol. I (Plenum, New York, 1974) p. 17.
12. A. G. EVANS and E. A. CHARLS, *J. Amer. Ceram. Soc.* **59** (1976) 371.
13. B. R. LAWN and E. R. FULLER, *J. Mater. Sci.* **10** (1975) 2016.
14. J. J. PETROVIC, L. A. JACOBSON, P. K. TALTY and A. K. VASUDEVAN, *J. Amer. Ceram. Soc.* **58** (1975) 113.
15. S.PALMQVIST, *Jernkontorets Ann.* **141** (1957) 300.
16. J. LANKFORD and D. L. DAVIDSON, *J. Mater. Sci.* **14** (1979) 1662.
17. K. L. JOHNSON, "Engineering Plasticity" (Cambridge University Press, London, 1968) p. 341.
18. C. J. STUDMAN and J. E. FIELD, *J. Phys. D, Appl. Phys.* **9** (1976) 857.
19. K. L. JOHNSON, *J. Mech. Phys.* **18** (1970) 115.
20. M. V. SWAIN and J. T. HAGAN, *J. Phys. D, Appl. Phys.* **9** (1976) 2201.
21. B. R. LAWN and R. WILSHAW, *J. Mater. Sci.* **10** (1975) 1049.
22. A. ARORA, D. B. MARSHALL and B. R. LAWN, *J. Non. Cryst. Sol.* **31** (1979) 415.
23. N.GANE and J. M. COX, *Philos. Mag.* **22** (1970) 881.
24. K. NIIHARA, *J. Mater. Sci. Lett.* **2** (1983) 221.
25. J. LANKFORD, *ibid.* **1** (1982) 493.

Received 22 March
and accepted 15 October 1984